Supporting Information

Elucidating the Role of Support Oxygen in the Water-Gas Shift Reaction Over Ceria-Supported Gold Catalysts Using *Operando* Spectroscopy

Christian Schilling, Christian Hess*

Eduard-Zintl-Institut für Anorganische und Physikalische Chemie, Technische Universität Darmstadt, Alarich-Weiss-Str. 8, 64287 Darmstadt, Germany

*hess@pc.chemie.tu-darmstadt.de

This document is the Accepted Manuscript version of a Published Work that appeared in final form in ACS Catalysis, copyright © 2018 American Chemical Society after peer review and technical editing by the publisher. To access the final edited and published work see https://doi.org/10.1021/acscatal.8b04536

Urheberrechtlich geschützt / In Copyright: https://rightsstatements.org/page/InC/1.0/

Catalyst Characterization

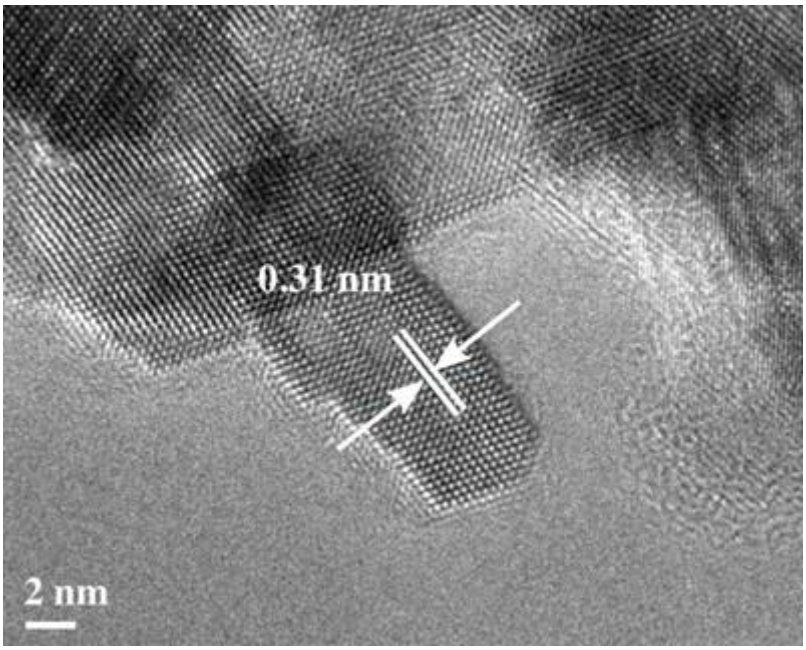

Figure S1: Transmission electron microscopy image of the synthesizes ceria support exposing the CeO_2(111) surface facet as shown by the characteristic lattice plane spacing in direction of the surface of 0.31 nm.

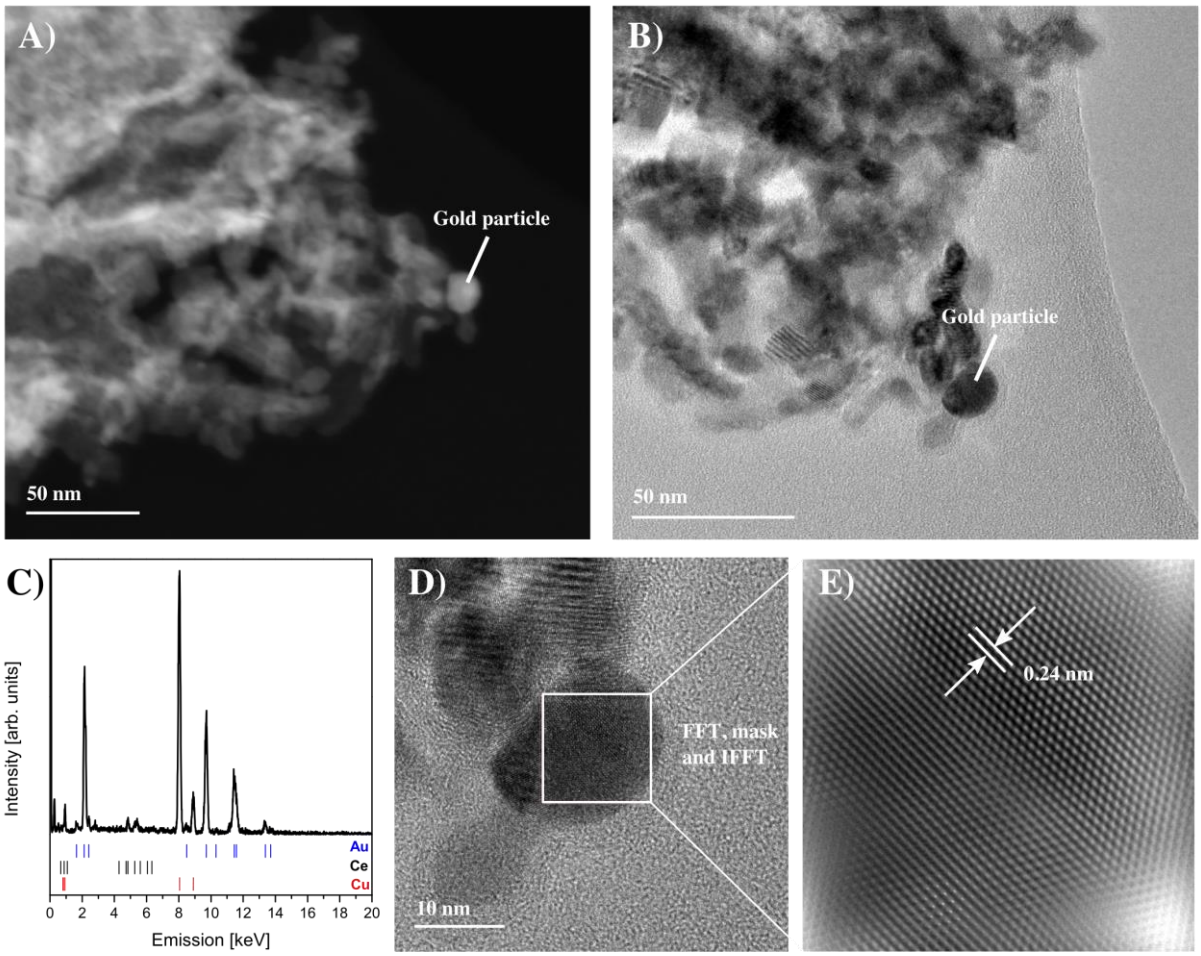

Figure S2: Transmission electron microscopic characterization of the 0.5 wt% Au/CeO_2 catalyst: A) STEM image, B) TEM image, C) point EDX of the gold particle, D) high-resolution TEM image of the gold particle, and E) corresponding inverse Fourier transform of the FFT plus applied mask to the Fourier transformed.

A)

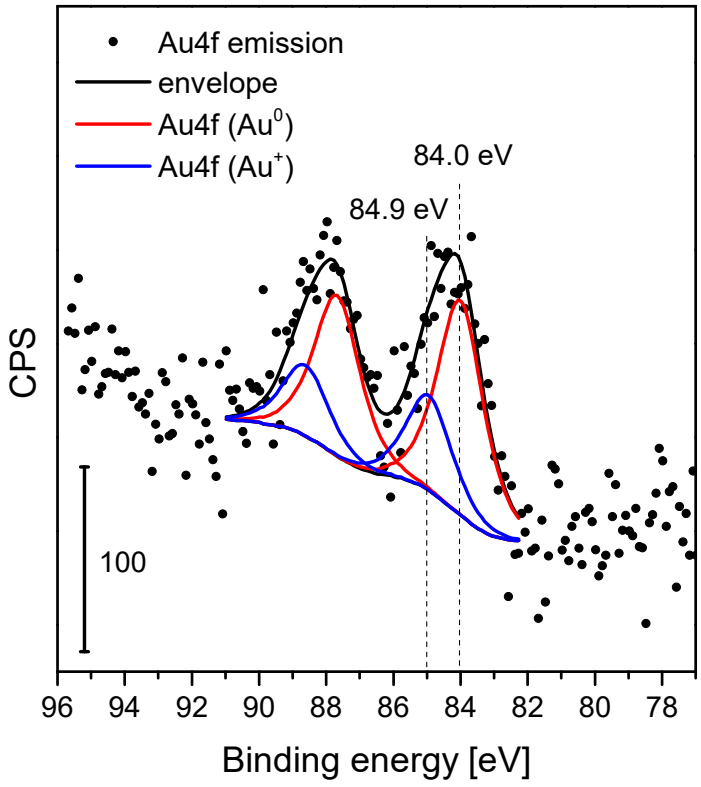
Au4f emission
envelope
Au4f (Au0)
Au4f (Au+)
84.0 eV
84.9 eV
CPS
100
96
94
92
90
88
86
84
82
80
78
Binding energy [eV]

B)

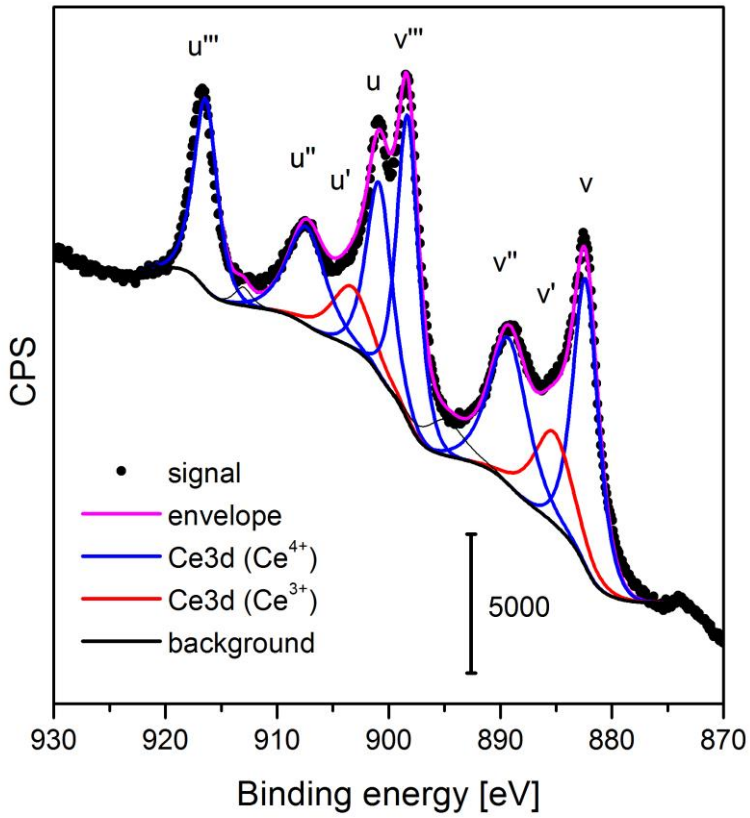

Figure S3: X-ray photoelectron spectra of the 0.5 wt% Au/CeO_2 catalyst. A) Au4f photoemission, B) Ce3d photoemission.

Catalysis

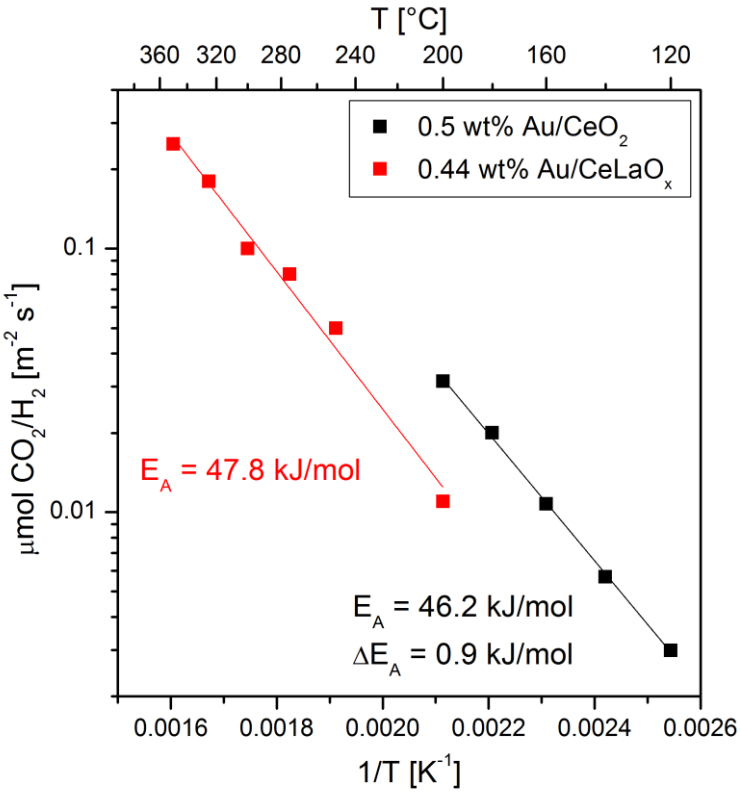

Figure S4: Arrhenius plot for the water-gas shift reaction (2 % CO, 10 % H_2O) over a 0.5 wt% Au/CeO_2 catalyst in a quartz tubular reactor with an online mass spectrometer described before (black squares). [1] For comparison the results by Fu *et al.* on a cyanide leached 0.44 wt% $Au/CeLaO_x$ (deposition precipitation) sample are shown (red squares). [2] It should be noted that the cyanide leached sample had the same conversion rate as a as prepared sample with 4.7 wt% Au/Ce LaO_x catalyst.

Density Functional Theory

The $Ce^{16}O_2(111)$ and $Ce^{18}O_2(111)$ surface

The frequency shifts of the modes at the $Ce^{18}O_2(111)$ surface (see Figure 4, red) with respect to a $Ce^{16}O_2(111)$ surface can be compared to those obtained by assuming isolated ^{140}Ce-$^{16/18}O$ harmonic oscillators (Δ), showing good agreement. The calculated frequency shifts from the harmonic oscillator model (Δ) compare well with the calculated values in Figure S6.

$$\nu(\text{long. harm}) = 225\ \text{cm}^{-1} * \sqrt{\frac{\frac{16*140}{16+140}}{\frac{18*140}{18+140}}} = 225\ \text{cm}^{-1} * 0.9488 = 213.5\ \text{cm}^{-1};$$

$$\Delta(\text{long.}) = 11.5\ \text{cm}^{-1}$$

$$\nu(\text{trans. harm}) = 363\ \text{cm}^{-1} * 0.9488 = 344.4\ \text{cm}^{-1};\ \Delta(\text{trans.}) = 18.6\ \text{cm}^{-1}$$

$$\nu(\text{F}_{2g}\ \text{harm}) = 423\ \text{cm}^{-1} * 0.9488 = 401.3\ \text{cm}^{-1};\ \Delta(\text{F}_{2g}\ \text{harm}) = 21.7\ \text{cm}^{-1}$$

$H_2O/CeO_2(111)$ interaction

The results for molecular (MS1) and dissociative water adsorption, i.e., hydroxyl pair formation at a $CeO_2(111)$ surface can be found in Table S1, resembling the calculated adsorption energies already published previously. [3] [4]

Table S1: Total Energy E_{tot} and adsorption energy of H_2O at the $CeO_2(111)$ surface with (2×2) periodicity with respect to $E_{\mathrm{ads,H_2O}}$ = 14.229 eV.

Structure	$\boldsymbol{E_{\mathrm{tot}}}$ **[eV]**	$\boldsymbol{E_{\mathrm{ads,H_2O}}}$ **[eV]**
$CeO_2(111)$	-291.330	
$CeO_2(111) + H_2O$ (MS1)	-306.094	-0.535
$CeO_2(111) + H_2O$ (HP1)	-306.072	-0.512
$CeO_{2-x}(111)$	-284.126	
$CeO_{2-x}(111) + H_2O$ (DD2)	-300.445	-2.024

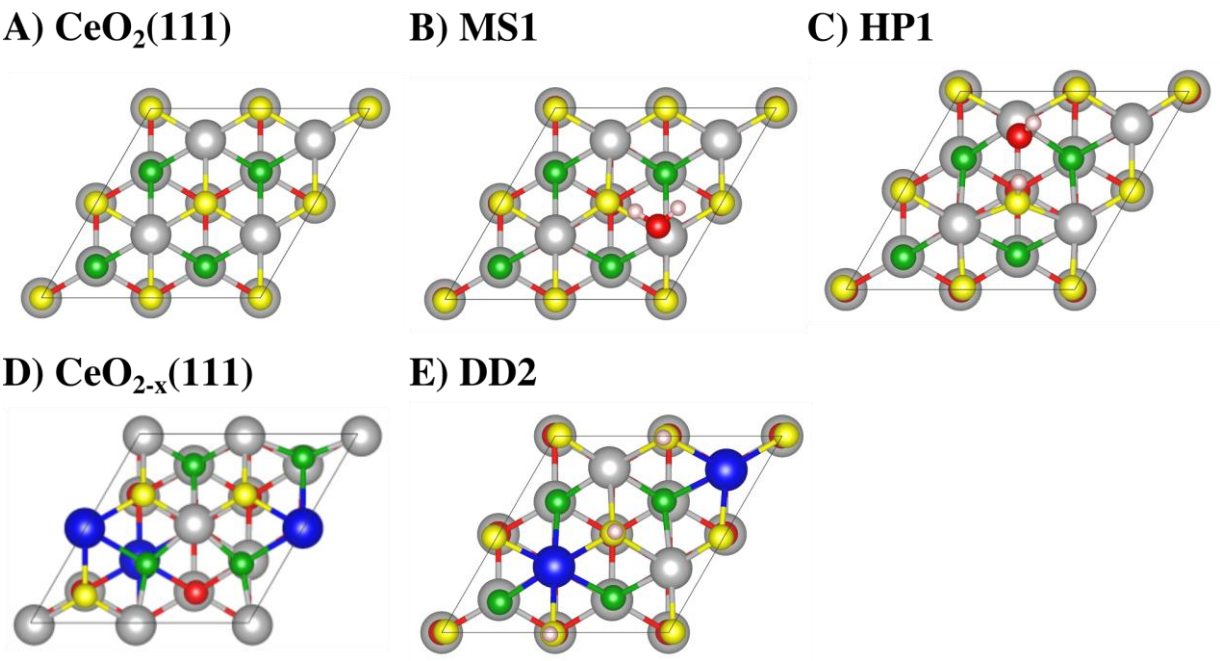

Figure S5: Top views of the A) oxidized $CeO_2(111)$ surface, B) molecular (MS1), and C) hydroxyl pair type (HP1) adsorption of H_2O at the $CeO_2(111)$ surface, D) the reduced $CeO_{2-x}(111)$ surface and E) dissociative adsorption at the $CeO_{2-x}(111)$ surface with (2×2) periodicity. Grey and blue balls represent Ce^{4+} and Ce^{3+} cations, yellow and green balls surface and subsurface oxygen, and red and light red balls represent oxygen (adsorbed water, hydroxy) and hydrogen, respectively.

Carbonate, hydrogen carbonate, and formate formation

The formation of carbonate and hydrogen carbonate species has been addressed extensively in the literature before by Vayssilov *et al.* [5] In addition, formate formation was analyzed by Lustemberg *et al.* [6] on the basis of temperature programmed surface reaction infrared spectroscopy and DFT together with statistical thermodynamics.

Table S2: Total energy of the carbonate, hydrogen carbonate and formate species at the CeO_2(111) surface calculated with (2×2) periodicity. *NNN* refers to the localization of the excess charge at Ce^{3+} in next nearest neighbor position with respect to the hydrogen carbonate or formate and *NN* refers to nearest neighbor position. *In plane* and *out plane* refers to Ce^{3+} localization in or out of the plane spanned by the hydrogen carbonate or formate species. *-b* refers to the protopn pointing to the surface in a hydrogen carbonate molecule.

Structure	$\boldsymbol{E_{tot}}$ **[eV]**	$\boldsymbol{E_{ads,CO_2}}$ **[eV]**
CeO_2(111)	-291.330	
CO_2/CeO_2(111)	-314.833	-0.515
CO_3H/CeO_{2-x}(111) NNN	-319.353	
CO_3H/CeO_{2-x}(111) NN, out plane	-319.196	
CO_3H/CeO_{2-x}(111) NN, in plane	-319.192	
CO_3H/CeO_{2-x}(111) NNN-b	-319.316	
CO_3H/CeO_{2-x}(111) NN, in plane-b	-319.151	
HCO_2/CeO_{2-x}(111) NNN	-311.994	
HCO_2/CeO_{2-x}(111) NN out plane	-311.829	
HCO_2/CeO_{2-x}(111) NN in plane	-311.818	
CO_2 gas	-22.988	
H_2 gas	-6.760	
CO gas	-14.806	

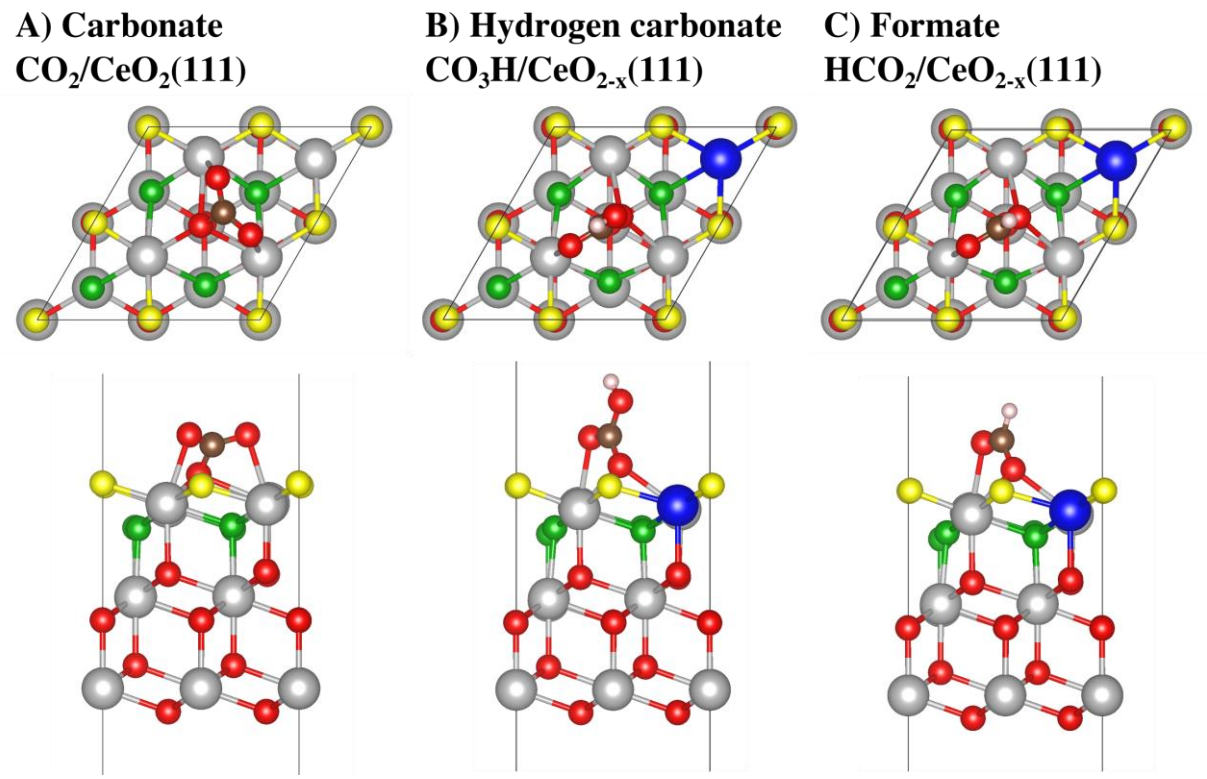

Figure S6: Top and side view of the most stable A) carbonate $CO_2/CeO_2(111)$, B) hydrogen carbonate $CO_3H/CeO_{2-x}(111)$, and C) formate $HCO_2/CeO_{2-x}(111)$ structures at a $CeO_2(111)$ surface with (2×2) periodicity. Grey and blue balls represent Ce^{4+} and Ce^{3+} cations, yellow and green balls surface and subsurface oxygen, whereas red, brown, and light red balls represent oxygen, carbon, and hydrogen as part of adsorbed species, respectively. Please note that oxygen below the first trilayer is represented by red balls.

In situ **Raman spectroscopy**

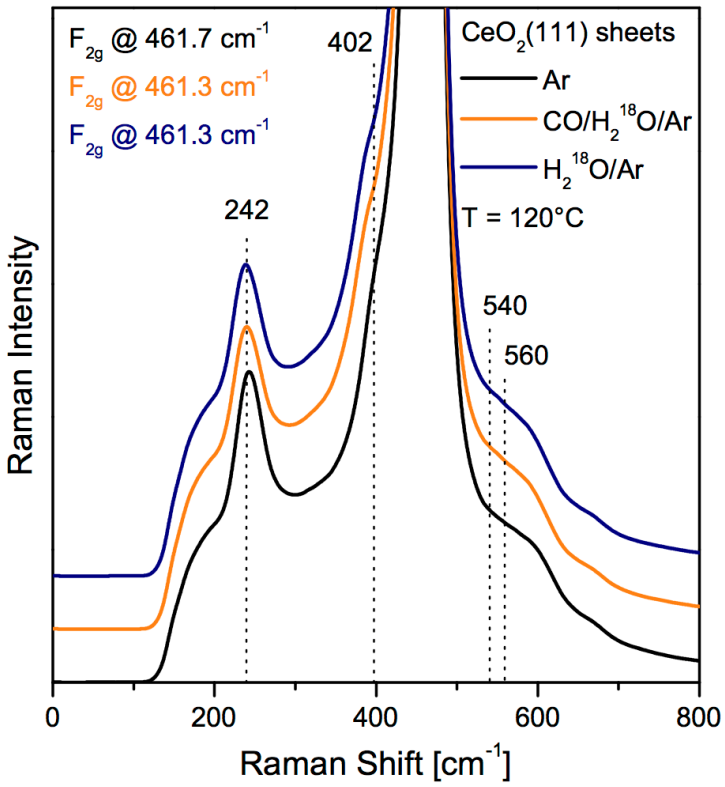

Figure S7. *In situ* Raman spectra of bare CeO_2 at 120°C during exposure to water-gas shift reaction conditions (2% CO, 8% $H_2{}^{18}O$, orange). For comparison spectra in Ar (black) and in 8% $H_2{}^{18}O$ (blue) are shown. The F_{2g} band is cut and the position of the F_{2g} band is given at the top left. Spectra are offset for clarity.

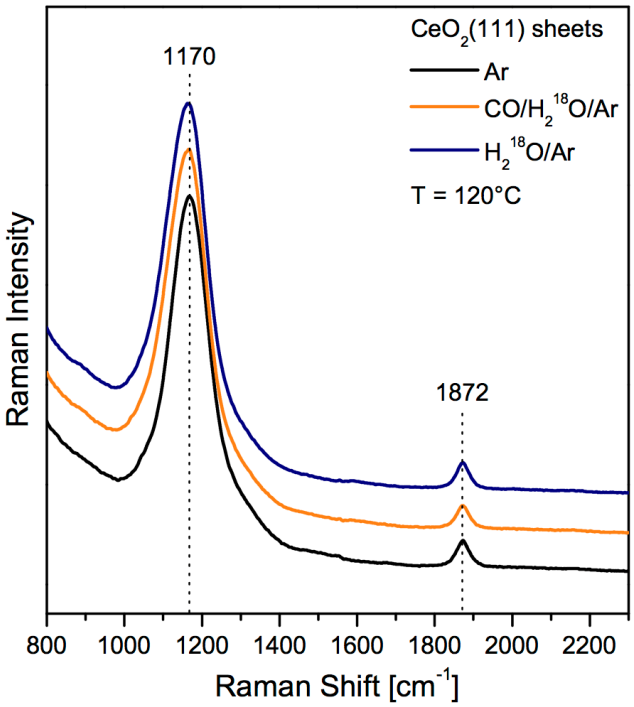

Figure S8. *In situ* Raman spectra of bare CeO_2 at 120℃ during exposure to water-gas shift reaction conditions (2% CO, 8% $H_2{}^{18}O$, orange). For comparison spectra in Ar (black) and in 8% $H_2{}^{18}O$ (blue) are shown. Spectra are offset for clarity.

Operando **UV-Vis spectroscopy**

In Figure S9, *operando* UV-Vis spectra of 0.5 wt% Au/CeO_2 during reaction are compared to *in situ* UV-Vis spectra of 0.5 wt% Au/CeO_2 in the presence of CO (2%) and H_2O (10%). Interestingly, the spectrum recorded under reaction conditions resembles that obtained in CO showing a strongly increased absorption between 450 - 1100 nm. This is attributed to reduced cerium ions of the ceria support rather than a gold plasmon as proposed before. [7] A contribution from the plasmon cannot be excluded here, but an assignment to a support reduction is corroborated by the *operando* Raman spectra discussed in the text. The spectrum after reaction in 8% H_2O resembles the spectrum of the Au/CeO_2 catalyst that was only exposed to 8% H_2O. Please note that a decrease of the absorption at ~350 nm is observed under reaction conditions and in CO that is regained in water atmosphere. The observed behavior appears to be characteristic of the band gap changes upon catalyst reduction and will be subject of further studies in the future.

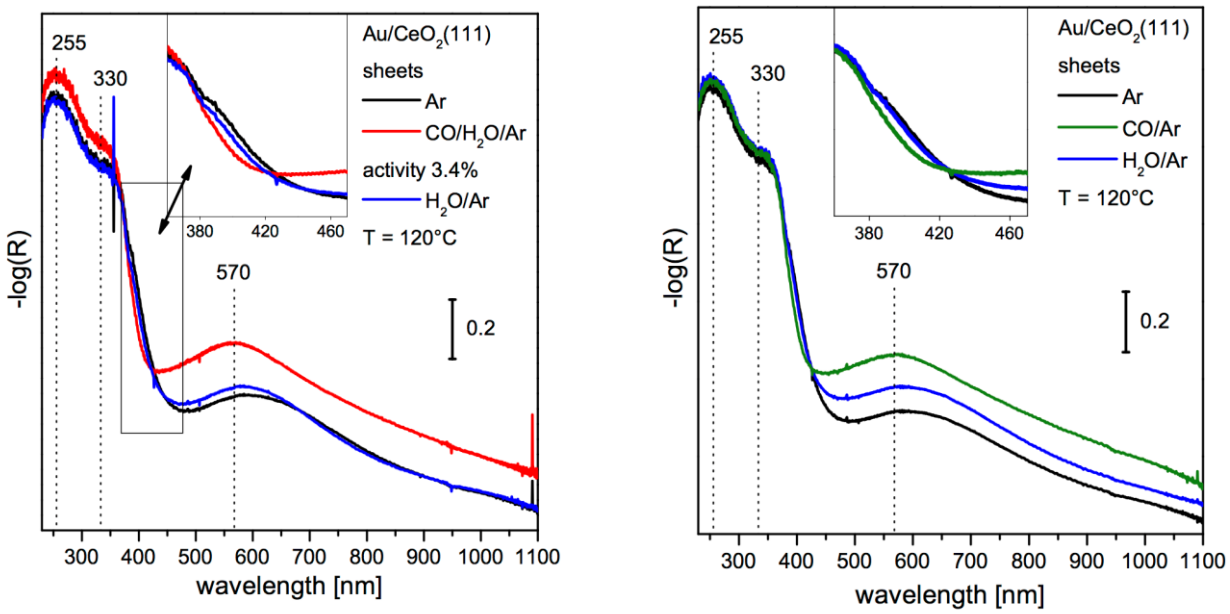

Figure S9. Left: *Operando* UV-Vis spectra of 0.5 wt% Au/CeO_2 at 120°C during water-gas shift reaction (2% CO, 8% H_2O, red). For comparison spectra in Ar prior reaction (black) and in 8% H_2O after reaction (blue) are shown. Right: *In situ* UV-Vis spectra of 0.5 wt% Au/CeO_2 at 120°C exposed to Ar (black), 2% CO (green), and 10% H_2O (blue). The insets give an enlarged view of the band gap regions.

Discussion of Raman sampling depth

In the following, the sampling depth of the visible (532 nm) Raman experiments in this study will be critically discussed in light of the results of the isotope experiments. One may assume that Raman spectroscopy probes a whole ceria nanoparticle of the Au/CeO_2 catalyst, as exposure of the Au/CeO_2 catalyst to $CO/H_2{}^{18}O/Ar$ leads to a more intense ^{18}O F_{2g} phonon band. However, after cooling the catalyst in argon stream the black dashed spectrum in Figure 9 is observed, which exhibits an F_{2g} band at the original ^{16}O position. In this context, it needs to be mentioned that during this treatment the catalyst was not exposed to $^{16}O_2$ or $H_2{}^{16}O$. The observed behavior allows us to draw the conclusion that Raman spectroscopy probes only the subsurface layers of the ceria particle where ^{18}O agglomerates during exposure to $CO/H_2{}^{18}O/Ar$, while a fraction of oxygen in the ceria particle remains ^{16}O. After exposure to $CO/H_2{}^{18}O/Ar$, equilibration of ^{18}O within the whole particle leads to a dilution of ^{18}O in the subsurface region and, as a consequence, a dominant ^{16}O F_{2g} phonon is measured by Raman spectroscopy. Based on the observations of the isotope experiments we therefore conclude that the sampling depth of Raman spectroscopy based on the F_{2g} phonon is confined to the subsurface region of the ceria particle rather than the whole ceria particle or the *bulk*. As shown in this study on the low temperature water-gas shift reaction at 120°C but also in a previous study on the room temperature CO oxidation [8] application of techniques such as Raman spectroscopy that enable to directly probe the dynamics of the ceria surface and the subsurface region plays an important role in understanding the mode of operation of Au/CeO_2 catalysts.

References

[1] Drochner, A.; Ohlig, D.; Knoche, S.; Gora, N.; Heid, M.; Menning, N.; Petzold, T.; Vogel, H. Activity Hysteresis during Cyclic Temperature-Programmed Reactions in the Partial Oxidation of Acrolein to Acrylic Acid. *Top. Catal.* **2016**, *59*, 1518-1532.

[2] Fu, Q.; Saltsburg, H.; Flytzani-Stephanopoulos, M. Active Nonmetallic Au and Pt Species on Ceria-Based Water-Gas Shift Catalysts. *Science* **2003**, *301*, 935-938.

[3] Molinari, M.; Parker, S. C.; Sayle, D. C.; Islam, M. S. Water Adsorption and its Effect on the Stability of Low Index Stoichiometric and Reduced Surfaces of Ceria. *J. Phys. Chem. C* **2012**, *116*, 7073-7082.

[4] Fernández-Torre, D.; Kośmider, K.; Carrasco, J.; Ganduglia-Pirovano, M. V.; Pérez, R. Insight into the Adsorption of Water on the Clean CeO_2(111) Surface with van der Waals and Hybrid Density Functionals. *J. Phys. Chem. C* **2012**, *116*, 13584-13593.

[5] Vayssilov, G. N.; Mihaylov, M.; Petkov, P. S.; Hadjiivanov, K. I.; Neyman, K. M. Reassignment of the Vibrational Spectra of Carbonates, Formates, and Related Surface Species on Ceria: A Combined Density Functional and Infrared Spectroscopy Investigation. *J. Phys. Chem. C* **2011**, 115, 23435-23454.

[6] Lustemberg, P. G.; Bosco, M. V.; Bonivardi, A.; Busnengo, H. F.; Ganduglia-Pirovano, M. V. Insights into the Nature of Formate Species in the Decomposition and Reaction of Methanol over Cerium Oxide Surfaces: A Combined Infrared Spectroscopy and Density Functional Theory Study. *J. Phys. Chem. C* **2015**, *119*, 21452-21464.

[7] Hernández, J. A.; Gómez, S. A.; Zepeda, T. A.; Fierro-González, J. C.; Fuentes, G. A. Insight into the Deactivation of Au/CeO_2 Catalysts Studied by In Situ Spectroscopy during the CO-PROX Reaction. *ACS Catal.* **2015**, *5*, 4003-4012.

[8] Schilling, C.; Hess, C. Real-Time Observation of the Defect Dynamics in Working Au/CeO_2 Catalysts by Combined Operando Raman/UV-Vis Spectroscopy. *J. Phys. Chem. C* **2018**, *122*, 2909-2917.